Electronic Research Archive

https://www.aimspress.com/journal/era

ERA, 33(9): 5401–5425.
DOI: 10.3934/era.2025242
Received: 21 July 2025
Revised: 23 August 2025
Accepted: 29 August 2025
Published: 12 September 2025

Research article

The weak Galerkin finite element method with or without stabilizer for the damped sine-Gordon equation and its reduced-order simulation

Senwen Deng[1], **Minfu Feng**[2], **Xi Li**[3] **and Li Zhang**[1,*]

[1] School of Mathematical Sciences, Sichuan Normal University, Chengdu 610066, China
[2] School of Mathematics, Sichuan University, Chengdu 610066, China
[3] School of Mathematical Sciences, Chengdu University of Technology, Chengdu 610059, China

* **Correspondence:** Email: lizhang_hit@163.com.

Abstract: In this work, an efficient scheme is proposed for the 2D damped sine-Gordon equation. The new scheme utilizes the unified weak Galerkin finite element method with or without stabilizer (UWG) in the spatial direction and the second-order explicit differentiation formula in the temporal direction. Both semi discrete schemes and fully discrete schemes are analyzed. First, we demonstrate the stability of the schemes. Subsequently, optimal error estimates are derived in the energy norm and the L^2 norm. Furthermore, by combining the proper orthogonal decomposition (POD) technique with the WG method, we develop a reduced-order algorithm, significantly improving computational efficiency. Finally, the theoretical results are validated by numerical experiments.

Keywords: damped sine-Gordon equation; weak Galerkin finite element method; with or without stabilizer; POD

1. Introduction

The sine-Gordon equation (SG), a classical model in nonlinear science, not only plays a crucial role in fields such as soliton theory [1], superconducting Josephson junctions [2], crystal dislocations [3], and topological solutions [4] in quantum field theory but also can be used to simulate different wave phenomena in areas like fluid mechanics [5] and optical fiber communications [6]. Thus, research on this equation has long been a focus of attention in the academic community. In this work, we consider the following 2D damped SG equation

$$u_{tt} + \beta u_t - \Delta u = \Psi(x, y)\sin(u) + f, \quad \text{in } \Omega \times (0, T], \tag{1.1}$$

with Dirichlet boundary

$$u(x, y, t) = 0, \quad \text{on } \partial\Omega \times (0, T], \tag{1.2}$$

and initial condition

$$u(x, y, 0) = g_0(x, y), \quad \text{in } \Omega, \tag{1.3}$$

$$u_t(x, y, 0) = g_1(x, y), \quad \text{in } \Omega, \tag{1.4}$$

where Ω is a bounded domain in $\mathbb{R}^2$ with Lipschitz-continuous boundary $\partial\Omega$. The nonnegative and bounded function $\Psi(\boldsymbol{x}) = \Psi(x, y)$ represents the Josephson current density, and the nonnegative real parameter $\beta \geq 0$ is referred to as the dissipative term. When $\beta = 0$, the equation is the undamped sine-Gordon equation. When $\beta > 0$, it reduces to the damped sine-Gordon equation. For simplicity, we denote $g_0(x, y)$ as $g_0(\boldsymbol{x})$ and $g_1(x, y)$ as $g_1(\boldsymbol{x})$ throughout this article.

Analytical solutions of the SG equation are often challenging to obtain due to complex boundary conditions, high-dimensional extensions, and strong nonlinear perturbations. Several numerical methods have been utilized to address the SG equation; for example Duan et al. [7] obtained key estimates via conformal symmetry for the wave–Klein–Gordon model. Farshid et al. [8] addressed 2D stochastic time-fractional cases on non-rectangular domains via finite difference and mesh–free methods, leveraging the flexibility of meshless techniques in complex geometries, and [9] proposed an algorithm for a nonlinear fractional hyperbolic wave model. Jiwari [10] further extended to multidimensional problems with barycentric rational interpolation and local radial basis functions, enhancing interpolation accuracy for high-dimensional systems. Beyond these, Ratas et al. [11] demonstrated the applicability of higher-order Haar wavelets on adaptive grids, Zhang et al. [12] constructed high-order Runge-Kutta schemes for parabolic types with maximum-principle preservation, and Wang and Huang [13] developed energy-conserving schemes for undamped systems, each targeting unique properties like adaptivity, stability, or structure preservation. Ahmed et al. [14] combined the WG method and the CN and Euler schemes to solve the SG equation and obtained the theoretical convergence orders.

The finite element method (FEM), widely used in engineering and physics, retains distinct advantages in local approximation and error analysis for the equation. Traditional FEM's limitations in addressing complex problems have spurred advanced extensions, notably the weak Galerkin (WG) method proposed by Wang and Ye for elliptic PDEs [15, 16]. Unlike classical FEM, WG replaces the gradient (∇) with a weak gradient (∇_w), enabling discontinuous basis functions within elements and across boundaries. This flexibility has driven its application to diverse PDEs, including the Brinkman equation [17], incompressible Navier-Stokes equations [18], biharmonic equations [19], linear elasticity problems [20], etc. And time-dependent systems like convection-diffusion equations [21, 22] and Klein-Gordon equations [23], etc. To simplify formulations and reduce complexity, stabilizer-free WG (SFWG) methods were developed [24–26] by enhancing polynomial degrees of weak gradient spaces, with successful applications to Stokes equations [27], time-fractional diffusion equations [28], and more. Recently, Wang and Ye [29] proposed a UWG framework for second-order elliptic problems, using a coefficient α to control the stabilizer.

Additionally, efficient computation of the WG method is a new direction in the research of the WG method. Proper orthogonal decomposition (POD) [30–32], a widely used model reduction technique, improves computational efficiency by extracting dominant features to build low-dimensional models while preserving key system characteristics. It has been combined with hybridized discontinuous Galerkin (HDG) [33], discontinuous Galerkin (DG) [34], DG–time stepping space–time finite element (TDG–STFE) [35], simplified weak Galerkin (SWG) [36], etc.

The goal of this work is to continue the investigation of UWG finite element methods for the damped SG equations (1.1)–(1.4). We use the UWG in the spatial direction and the central differences formula in the temporal direction. The stability and convergence analysis of the schemes are provided. We obtain the optimal error estimates in the energy norm and the L^2 norm. To improve the computational efficiency of the proposed schemes, we develop a fast and effective reduced-order algorithm by combining it with the POD method. These theoretical findings are verified through two numerical examples. There are two key differences between the current methods used by us and the method proposed in [14]. One is that the author proposed a WG method with a stabilizer in [14]. The other is that we employ an explicit scheme similar to the one used in [37] that achieves the same efficient convergence rate as the CN scheme.

The structure of this article is as follows. Section 2 introduces basic notation and relevant lemmas for the WG method. Section 3 presents the semi-discrete form of the damped sine-Gordon equation, along with error estimates in semi-norm and L^2 norm. Section 4 develops and analyzes the fully discrete scheme. Section 5 integrates the POD method with the UWG to form a reduced-order model. Finally, Section 6 provides numerical examples to verify the model's effectiveness. And Appendix A lists the abbreviations.

2. Preliminary

2.1. Notations and definitions

We use $H^s(D)$ to denote the standard Sobolev space of order s, where $s \geq 0$ and $D \in \mathbb{R}^2$. Use $(\cdot,\cdot)_{s,D}$, $\|\cdot\|_{s,D}$ and $|\cdot|_{s,D}$ denote the inner product, norm and seminorm. Particularly, when $s = 0$, we denote $H^s(D)$ as $L^2(D)$, use $(\cdot,\cdot)_D$, $\|\cdot\|_D$ and $|\cdot|_D$ in place of $(\cdot,\cdot)_{s,D}$, $\|\cdot\|_{s,D}$ and $|\cdot|_{s,D}$. For simplicity, we omit the subscript D when $D = \Omega$. Besides, the constant C may take different values.

Now, define the space $H^l(0,T;H^s(\Omega))$ by

$$H^l(0,T;H^s\Omega) = \{\omega \in H^s(\Omega); \sum_{0\leq i\leq l}\int_0^T \|\frac{\partial^i\omega(t)}{\partial t^i}\|^2_{s,\Omega}dt < \infty\},$$

with norm

$$\|\omega\|^2_{H^l(H^s(\Omega))} = \sum_{0\leq i\leq l}\int_0^T \|\frac{\partial^i\omega(t)}{\partial t^i}\|^2_{s,\Omega}dt,$$

if $0 \leq l \leq \infty$ and

$$\|\omega\|^2_{H^l(H^s(\Omega))} = \int_0^T \|\omega(t)\|^2_{s,\Omega}dt,$$

if $l = 0$.

Let $\mathcal{T}_h = \cup\{T\}$ be a shape-regular simplicial partition of the domain Ω, and $\mathcal{E}_h = \cup\{\partial T\}$ be the set of all edges of $T \in \mathcal{T}_h$, $\mathcal{E}_h^0 = \mathcal{E}_h \setminus \partial\Omega$ be the set of all interior edge. Denote the diameter of the each element $T \in \mathcal{T}_h$ by h_T, and $h = \max_{T\in\mathcal{T}_h} h_T$ for $\mathcal{T}_h$.

For any element $T \in \mathcal{T}_h$, the space of weak function $W(T)$ is defined on T as:

$$W(T) = \{v = \{v_0, v_b\} : v_0 \in L^2(T), v_b \in L^2(\partial T)\}, \tag{2.1}$$

if $v \in H^1(\Omega)$, then $v = \{v, v\}$.

On each element T, for any integer $k \geq 0$, let $P_k(T)$ be the space of all polynomials of degree no more than k. Then the weak Galerkin finite element space V_h is defined as

$$V_h = \{v = \{v_0, v_b\} : v_0 \in P_k(T), v_b \in P_k(E), \forall T \in \mathcal{T}_h, \forall E \in \mathcal{E}_h\}, \tag{2.2}$$

and its subspace V_h^0 is defined as

$$V_h^0 = \{v : v \in V_h, v_b = 0 \text{ on } \partial\Omega\}. \tag{2.3}$$

Definition 2.1. *[29] For $v = \{v_0, v_b\} \in V_h$, its weak gradient $\nabla_w v \in [P_j(T)]^2$ in element T is the unique solution satisfying*

$$(\nabla_w v, \boldsymbol{q})_T = -(v_0, \nabla \cdot \boldsymbol{q})_T + \langle v_b, \boldsymbol{q} \cdot \boldsymbol{n}\rangle_{\partial T}, \quad \forall \boldsymbol{q} \in [P_j(T)]^2, \tag{2.4}$$

where $\boldsymbol{n}$ is unit external normal vector on ∂T, and $j \geq k + n - 1$, n represents the number of element edges.

Next, we introduce three L^2 projection operators. Let Q_0 from $L^2(T)$ onto $P_k(T)$ for all $T \in \mathcal{T}_h$ and Q_b from $L^2(E)$ to $P_k(E)$ for all $E \in \mathcal{E}_h$, respectively. Combined projection operator $Q_h v = \{Q_0 v, Q_b v\} \in V_h$, and $\mathbb{Q}_h$ from $[L^2(T)]^2$ onto $[P_j(T)]^2$ for each $T \in \mathcal{T}_h$.

Lemma 2.1. *[16] Let $u \in H^{k+1}(\Omega)$, $k \geq 0$; there is a constant $C > 0$ such that $Q_h u$ satisfies the following properties:*

$$\|u - Q_0 u\|_T^2 + h^2 \|\nabla(u - Q_0 u)\|_T^2 \leq C h^{2(k+1)} \|u\|_{k+1}^2, \tag{2.5}$$

$$\|\nabla u - \mathbb{Q}_h \nabla u\|_T^2 + h^2 |\nabla u - \mathbb{Q}_h \nabla u|_{1,T}^2 \leq C h^{2k} \|u\|_{k+1}^2. \tag{2.6}$$

Lemma 2.2. *[38] For $u \in H^1(\Omega)$, and $\boldsymbol{q} \in [P_j(T)]^2$, then for any $T \in \mathcal{T}_h$*

$$(\nabla_w(Q_h u), \boldsymbol{q})_T = (\mathbb{Q}_h \nabla u, \boldsymbol{q})_T + (u - Q_0 u, \nabla \cdot \boldsymbol{q})_T - \langle u - Q_b u, \boldsymbol{q} \cdot \boldsymbol{n}\rangle_{\partial T}, \tag{2.7}$$

$$\nabla_w u = \mathbb{Q}_h \nabla u. \tag{2.8}$$

2.2. The UWG scheme

The variational formulation of the SG equations (1.1)–(1.4) is to seek $u \in L^2(0, T; H_0^1(\Omega))$

$$(u_{tt}, v) + \beta(u_t, v) + (\nabla u, \nabla v) = (\Psi(\boldsymbol{x}) \sin(u), v) + (f, v), \quad \forall v \in H_0^1(\Omega), t \in (0, T]. \tag{2.9}$$

Define the semi-discrete UWG scheme of SG equations (1.1)–(1.4) as follow:
Find $U = \{U_0, U_b\} \in L^2(0, T; V_h^0)$ satisfying

$$\begin{cases} ((U_0)_{tt}, v_0) + \beta((U_0)_t, v_0) + A_{\alpha w}(U, v) = (\Psi(\boldsymbol{x}) \sin(U_0), v_0) + (f, v_0), \quad \forall v \in V_h^0, \\ U(0) = Q_h g_0, U_t(0) = Q_h g_1, \end{cases} \tag{2.10}$$

here

$$A_{\alpha w}(U, v) = (\nabla_w U, \nabla_w v) + \alpha S(U, v),$$

$$S(u, v) = \sum_{T \in \mathcal{T}_h} h_T^{-1} \langle u_0 - u_b, v_0 - v_b\rangle_{\partial T},$$

where $\alpha = 0$ or 1. For any $v_h = \{v_0, v_b\} \in V_h$, we define a semi-norm

$$|||v_h|||^2 = A_{\alpha w}(v_h, v_h) = (\nabla_w v_h, \nabla_w v_h)_{\mathcal{T}_h} + \alpha S(v_h, v_h), \tag{2.11}$$

we known that $|||\cdot|||$ is a norm in V_h^0. For detailed proof, please refer to Lemma 3 of [29].

Lemma 2.3. *[29] When $j \geq k+n-1$, for any $v_h = \{v_0, v_b\} \in V_h$, we have*

$$\sum_{T\in\mathcal{T}_h} h^{-1}\|v_0 - v_b\|_{\partial T}^2 \leq C \sum_{T\in\mathcal{T}_h} \|\nabla_w v\|_T^2. \tag{2.12}$$

where C is a positive constant independent of h.

Lemma 2.4. *For any $v \in V_h^0$, we have*

$$|||\, v||| \leq C\|v\|_{1,h}, \tag{2.13}$$

where C is a positive constant independent of h.

Proof. According to [24], when $\alpha = 0$, there exist two constants, C_1 and C_2 such that

$$C_1\|v\|_{1,h} \leq |||v||| \leq C_2\|v\|_{1,h},$$

where $\|v\|_{1,h} = (\sum_{T\in\mathcal{T}_h}(\|\nabla v_0\|_T^2 + h^{-1}\|v_0 - v_b\|_{\partial T}^2))^{\frac{1}{2}}$. Combined with Lemma 2.3, we get $|||v||| \leq C\|v\|_{1,h}$ whether $\alpha = 0$ or 1.

3. Semi-discrete scheme

3.1. Stability of semi-discrete scheme

In this section, we will give a stability analysis of semi-discrete scheme (2.10).

Theorem 3.1. *Let $U \in L^2(0,T;V_h^0)$ be the solution of problem (2.10) and $f \in L^2(\Omega\times(0,T])$. Then*

$$\|(U_0)_t\|^2 + |||U|||^2 \leq \|(U_0)_t(0)\|^2 + |||U(0)\,|||^2 + C\int_0^T \|f\|^2 dt, \tag{3.1}$$

where C is a positive constant independent of h.

Proof. Taking $v = U_t$ in the first equation of (2.10), we have

$$((U_0)_{tt}, (U_0)_t) + \beta((U_0)_t, (U_0)_t) + A_{\alpha w}(U, U_t) = (\Psi(\boldsymbol{x})\sin(U_0), (U_0)_t) + (f, (U_0)_t).$$

By Cauchy–Schwarz, Young's inequalities, and $\|\sin(u)\| \leq \|u\|$, we have

$$\frac{1}{2}\frac{d}{dt}\|(U_0)_t\|^2 + \beta\|(U_0)_t\|^2 + \frac{1}{2}\frac{d}{dt}\,|||\,U|||^2 \leq C\|U_0\|^2 + \frac{\beta}{2}\|(U_0)_t\|^2 + C\|f\|^2 + \frac{\beta}{2}\|(U_0)_t\|^2.$$

Integrating with respect to time and using extended Gronwall's inequality, we get

$$\frac{1}{2}\|(U_0)_t\|^2 + \frac{1}{2}\,|||\,U|||^2 \leq \frac{1}{2}\|(U_0)_t(0)\|^2 + \frac{1}{2}\,|||\,U(0)\,|||^2 + C\int_0^T \|f\|^2 dt.$$

The conclusion readily follows from the above inequality.

3.2. Error estimates in the energy norm

In this section, we will give an error estimate of semi-discrete scheme (2.10) with $|||\cdot|||$. Before analysis, let $u - U = u - Q_h u + Q_h u - U := \eta_h + e_h$, where $e_h = \{Q_0 u - U_0, Q_b u - U_b\} = \{e_0, e_b\}$.

Lemma 3.2. *[29] For $v = \{v_0, v_b\} \in V_h^0$, let $u \in H^1(0, T; H^{k+1})$ be the solution of problems (1.1)–(1.4), then*

$$\begin{aligned}&(Q_0 u_{tt}, v_0) + \beta(Q_0 u_t, v_0) + (\nabla_w Q_h u, \nabla_w v)\\ =&(\Psi(\boldsymbol{x})\sin(u), v_0) + (f, v_0) + l_1(u, v) + l_2(u, v) + l_3(u, v).\end{aligned} \tag{3.2}$$

Where

$$\begin{aligned} l_1(u, v) &= \sum_{T\in\mathcal{T}_h} \langle (\nabla u - \mathbb{Q}_h \nabla u)\cdot \mathbf{n}, v_0 - v_b\rangle_{\partial\mathcal{T}_h},\\ l_2(u, v) &= \sum_{T\in\mathcal{T}_h} \langle Q_b u - u, \nabla_w v\cdot \mathbf{n}\rangle_{\partial\mathcal{T}_h},\\ l_3(u, v) &= \sum_{T\in\mathcal{T}_h} ((u - Q_0 u), \nabla\cdot\nabla_w v)_{\mathcal{T}_h}.\end{aligned}$$

Lemma 3.3. *For any $u \in H^{k+1}(\Omega)$ and $v = \{v_0, v_b\} \in V_h^0$, we have*

$$|l_1(u, v)| \le Ch^k \|u\|_{k+1} \,|||\, v|||, \tag{3.3}$$

$$|l_2(u, v)| \le Ch^k \|u\|_{k+1} \,|||\, v|||, \tag{3.4}$$

$$|l_3(u, v)| \le Ch^k \|u\|_{k+1} \,|||\, v|||, \tag{3.5}$$

$$|S(Q_h u, v)| \le Ch^k \|u\|_{k+1} \,|||\, v|||, \tag{3.6}$$

$$|(\Psi(\boldsymbol{x})(\sin(u) - \sin(U)), v_0)| \le Ch^{k+1}\|u\|_{k+1}\|v_0\| + \|e_0\|\|v_0\|. \tag{3.7}$$

Proof. Equations (3.3)–(3.6) can be obtained by referring to the proof in [29].

By Cauchy–Schwarz, the Lipschitz continuity of $\sin(u)$, and Lemma 2.1, we have

$$\begin{aligned}|(\Psi(\boldsymbol{x})(\sin(u) - \sin(U)), v_0)| &\le C\|U - u\|\|v_0\|\\ &\le \|Q_0 u - u\|\|v_0\| + \|U - Q_0 u\|\|v_0\|\\ &\le Ch^{k+1}\|u\|_{k+1}\|v_0\| + \|e_0\|\|v_0\|.\end{aligned}$$

The proof is completed.

Lemma 3.4. *Assume $u \in H^1(0, T; H^{k+1})$ and $v \in L^2(0, T, V_h)$; then for any $t \in (0, T]$ we have*

$$\begin{aligned}\Big|\int_0^t l_1(u, \frac{\partial v}{\partial t})dt\Big| \le& Ch^{2k}(\|u\|_{k+1}^2 + \|u(0)\|_{k+1}^2 + \int_0^t \|\frac{\partial u}{\partial t}\|_{k+1}^2 dt)\\ &+ C(|||v|||^2 + |||v(0)|||^2) + C\int_0^t |||v|||^2\, dt,\end{aligned} \tag{3.8}$$

$$\begin{aligned}\Big|\int_0^t l_2(u, \frac{\partial v}{\partial t})dt\Big| \le& Ch^{2k}(\|u\|_{k+1}^2 + \|u(0)\|_{k+1}^2 + \int_0^t \|\frac{\partial u}{\partial t}\|_{k+1}^2 dt)\\ &+ C(|||v|||^2 + |||v(0)|||^2) + C\int_0^t |||v|||^2\, dt,\end{aligned} \tag{3.9}$$

$$
\begin{aligned}
|\int_0^t l_3(u,\frac{\partial v}{\partial t})dt| \leq & Ch^{2k}(\|u\|_{k+1}^2+\|u(0)\|_{k+1}^2+\int_0^t\|\frac{\partial u}{\partial t}\|_{k+1}^2dt)\\
&+C(|||v|||^2+|||v(0)|||^2)+C\int_0^t|||v|||^2\,dt,
\end{aligned}
\tag{3.10}
$$

$$
\begin{aligned}
|\int_0^t S(Q_hu,\frac{\partial v}{\partial t})dt| \leq & Ch^{2k}(\|u\|_{k+1}^2+\|u(0)\|_{k+1}^2+\int_0^t\|\frac{\partial u}{\partial t}\|_{k+1}^2dt)\\
&+C(|||v|||^2+|||v(0)|||^2)+C\int_0^t|||v|||^2\,dt,
\end{aligned}
\tag{3.11}
$$

$$
\begin{aligned}
&|\int_0^t(\Psi(\boldsymbol{x})(\sin(U)-\sin(u)),\frac{\partial v_0}{\partial t})dt|\\
\leq & Ch^{2(k+1)}(\|u\|_{k+1}^2+\|u(0)\|_{k+1}^2+\int_0^t\|\frac{\partial u}{\partial t}\|_{k+1}^2dt)+C(\|e_0\|^2+\|v_0\|^2)\\
&+C(\int_0^t\|v_0\|^2dt+\int_0^t\|\frac{\partial e_0}{\partial t}\|^2dt).
\end{aligned}
\tag{3.12}
$$

Proof. By Lemma 3.3, we use integration by parts to get

$$
\begin{aligned}
&|\int_0^t l_1(u,\frac{\partial v}{\partial t})dt|\\
=&|l_1(u,v)(t)-l_1(u,v)(0)-\int_0^t l_1(\frac{\partial u}{\partial t},v)dt|\\
\leq & Ch^k\|u\|_{k+1}\,|||v|||+Ch^k\|u(0)\|_{k+1}\,|||v(0)|||+\int_0^t Ch^k\|\frac{\partial u}{\partial t}\|_{k+1}\,|||v|||\,dt\\
\leq & Ch^{2k}(\|u\|_{k+1}^2+\|u(0)\|_{k+1}^2+\int_0^t\|\frac{\partial u}{\partial t}\|_{k+1}^2dt)+C(|||v|||^2+|||v(0)|||^2)+C\int_0^t|||v|||^2\,dt.
\end{aligned}
$$

Then we can prove (3.8)–(3.11) by the same approach. The proof for (3.12) is more involved but follows the same approach. The details are as follows.

$$
\begin{aligned}
&|\int_0^t(\Psi(\boldsymbol{x})(\sin(U)-\sin(u)),\frac{\partial v_0}{\partial t})dt|\\
\leq & |(\Psi(\boldsymbol{x})(\sin(U)-\sin(u)),v_0)(t)-(\Psi(\boldsymbol{x})(\sin(U)-\sin(u)),v_0)(0)\\
&-\int_0^t(\Psi(\boldsymbol{x})(\frac{\partial\sin(U)-\sin(u))}{\partial t},v_0)dt|\\
\leq & Ch^{k+1}\|u\|_{k+1}\|v_0\|(t)+\|e_0\|\|v_0\|(t)+Ch^{k+1}\|u\|_{k+1}\|v_0\|(0)+\|e_0\|\|v_0\|(0)\\
&+\int_0^t Ch^{k+1}\|\frac{\partial u}{\partial t}\|_{k+1}\|v_0\|+\|\frac{\partial e_0}{\partial t}\|\|v_0\|dt\\
\leq & Ch^{2(k+1)}(\|u\|_{k+1}^2+\|u(0)\|_{k+1}^2+\int_0^t\|\frac{\partial u}{\partial t}\|_{k+1}^2dt)+C(\|e_0\|^2+\|v_0\|^2)\\
&+C(\int_0^t\|v_0\|^2dt+\int_0^t\|\frac{\partial e_0}{\partial t}\|^2dt).
\end{aligned}
\tag{3.13}
$$

The proof is completed.

Theorem 3.5. *Assume u and $U \in V_h^0$ are the solutions of (1.1)–(1.4) and (2.10), respectively. Moreover, for a fixed time $t \in (0, T]$, if $u \in L^2(0, T; H^{k+1}(\Omega))$ and $u_t \in L^2(0, T; H^{k+1}(\Omega))$, then we have*

$$|||\, e_h|||^2 \le Ch^{2k}(\|U\|_{k+1}^2 + \|U(0)\|_{k+1}^2 + \int_0^t \|\frac{\partial U}{\partial t}\|_{k+1}^2 dt), \tag{3.14}$$

where C is a positive constant independent of h.

Proof. Subtracting the first equation of (2.10) from (3.2) add stabilizer at both sides, we get the following error equation:

$$\begin{aligned} &((e_0)_{tt}, v_0) + \beta((e_0)_t, v_0) + (\nabla_w e_h, \nabla_w v) + \alpha S(e_h, v) \\ =&(\Psi(\boldsymbol{x})(\sin(u) - \sin(U)), v_0) + l_1(u, v) + l_2(u, v) + l_3(u, v) + \alpha S(Q_h u, v). \end{aligned} \tag{3.15}$$

Taking $v = (e_h)_t$ in (3.15), we have

$$\begin{aligned} &\frac{1}{2}\frac{d}{dt}\|(e_0)_t\|^2 + \beta\|(e_0)_t\|^2 + \frac{1}{2}\frac{d}{dt}\,|||\, e_h|||^2 \\ =&(\Psi(\boldsymbol{x})(\sin(u) - \sin(U)), (e_0)_t) + l_1(u, (e_h)_t) + l_2(u, (e_h)_t) + l_3(u, (e_h)_t) + \alpha S(Q_h u, (e_h)_t). \end{aligned}$$

Integrating both sides over time t and combining $e_h(0) = (e_h)_t(0) = 0$, we have

$$\begin{aligned} &\frac{1}{2}\|(e_0)_t\|^2 + \beta\int_0^t \|(e_0)_t\|^2 dt + \frac{1}{2}\,|||\, e_h|||^2 \\ =&\int_0^t ((\Psi(\boldsymbol{x})(\sin(u) - \sin(U)), (e_0)_t) + l_1(u, (e_h)_t) + l_2(u, (e_h)_t) + l_3(u, (e_h)_t) + \alpha S(Q_h u, (e_h)_t))dt. \end{aligned}$$

Applying Lemma 3.4, there exists a constant C, such that

$$\begin{aligned} &\frac{1}{2}\|(e_0)_t\|^2 + \beta\int_0^t \|(e_0)_t\|^2 dt + \frac{1}{2}\,|||\, e_h|||^2 \\ \le&Ch^{2k}(\|U\|_{k+1}^2 + \|U(0)\|_{k+1}^2 + \int_0^t \|\frac{\partial U}{\partial t}\|_{k+1}^2 dt) + \frac{1}{4}\,|||\, e_h\,|||^2 + C\int_0^t |||e_h\,|||^2\, dt \\ &+ \frac{1}{2}\|(e_0)_t\|^2 + \beta\int_0^t \|(e_0)_t\|^2 dt. \end{aligned}$$

Finally, using Gronwall's inequality, we get

$$|||e_h|||^2 \le Ch^{2k}(\|U\|_{k+1}^2 + \|U(0)\|_{k+1}^2 + \int_0^t \|\frac{\partial U}{\partial t}\|_{k+1}^2 dt).$$

We get the conclusion.

3.3. Error estimates in the L^2 norm

In this section, we will give an error estimate of semi-discrete scheme (2.10) with $\|\cdot\|$. Before analysis, let us introduce the elliptic projection and its properties.

Definition 3.1. *The elliptic projection $R_h : H^2(\Omega) \cap H_0^1 \to V_h^0$ as*

$$A_{\alpha w}(R_h u, v_h) = (-\nabla \cdot (\nabla u), v_h), \quad \forall v_h \in V_h, \tag{3.16}$$

with $R_h u(0) = Q_h u(0)$, $R_h u_t(0) = Q_h u_t(0)$.

Lemma 3.6. *[39] If $u \in H^{k+1}(\mathcal{T}_h)$, then it holds*

$$\|Q_h u(t) - R_h u(t)\|^2 \le C h^{2(k+1)} \|u(t)\|_{k+1}^2,$$

with the help of elliptical projection, the error $e_h = Q_h u - U$ can be further divided into

$$e_h(t) = Q_h u(t) - U(t) = Q_h u(t) - R_h u - (U(t) - R_h u) := \rho(t) - \xi(t).$$

Theorem 3.7. *Assume u and $U \in V_h^0$ are the solutions of (1.1) and (2.10), respectively. Moreover, for a fixed time $t \in (0, T]$ if $u \in L^2(0, T; H^{k+1}(\Omega))$ and $u_t \in L^2(0, T; H^{k+1}(\Omega))$, then we have*

$$\|\xi_0(t)\|^2 \le C h^{2(k+1)} (\|(u_0)_t\|_{k+1}^2 + \|u_0\|_{k+1}^2 + \|u\|_{k+1}^2 + \|u(0)\|_{k+1}^2). \tag{3.17}$$

where C is a positive constant independent of h.

Proof. Multiplying the test function $v_0 \in V_h^0$ in (1.1), from (3.16) and Green's formula, we have

$$(Q_0 u_{tt}, v_0) + \beta(Q_0 u_t, v_0) + A_{\alpha w}(R_h u, v_h) = (\Psi(\boldsymbol{x}) \sin(u), v_0) + (f, v_0). \tag{3.18}$$

Subtracting (2.10) from (3.18), we have the following error equation:

$$((\xi_0)_{tt}, v_0) + \beta((\xi_0)_t, v_0) + A_{\alpha w}(\xi, v_h) = ((\rho_0)_{tt}, v_0) + \beta((\rho_0)_t, v_0) - \frac{d}{dt}(G, v_0) + (G, (v_0)_t), \tag{3.19}$$

where $G(t) = \Psi(\boldsymbol{x}) \int_0^t (\sin(u) - \sin(U))(s) ds, 0 \le t \le T$.

For $\theta \in (0, T]$ define $\overline{\xi}$ as:

$$\overline{\xi}(\cdot, t) = \int_t^\theta \xi(\cdot, s) ds \quad 0 \le t \le T. \tag{3.20}$$

It is easy to see that $\overline{\xi}(\theta) = 0$, $\overline{\xi_t} = -\xi(\cdot, t), 0 \le t \le T$.

Taking $v_h = \overline{\xi}$ in (3.19), we have

$$((\xi_0)_{tt}, \overline{\xi_0}) + \beta((\xi_0)_t, \overline{\xi_0}) + A_{\alpha w}(\xi, \overline{\xi}) = ((\rho_0)_{tt}, \overline{\xi_0}) + \beta((\rho_0)_t, \overline{\xi_0}) - \frac{d}{dt}(G, \overline{\xi_0}) + (G, \overline{(\xi_0)_t}).$$

Integrating with respect to t from 0 to θ , we have

$$\begin{aligned} &\int_0^\theta ((\xi_0)_{tt}, \overline{\xi_0}) dt + \int_0^\theta \beta((\xi_0)_t, \overline{\xi_0}) dt + \int_0^\theta A_{\alpha w}(\xi, \overline{\xi}) dt \\ &= \int_0^\theta ((\rho_0)_{tt}, \overline{\xi_0}) dt + \int_0^\theta \beta((\rho_0)_t, \overline{\xi_0}) dt - \int_0^\theta \frac{d}{dt}(G, \overline{\xi_0}) dt + \int_0^\theta (G, \overline{(\xi_0)_t}) dt. \end{aligned}$$

Then integrate by parts over t, and notice $\xi(0) = \rho(0) = 0$, $\xi_t(0) = \rho_t(0) = 0$, we have

$$\begin{aligned}
&-\int_0^\theta ((\xi_0)_t, \overline{(\xi_0)_t})dt - \beta\int_0^\theta (\xi_0, (\overline{\xi_0})_t)dt + \int_0^\theta A_{\alpha w}(\xi, \overline{\xi})dt \\
=&-\int_0^\theta ((\rho_0)_t, \overline{(\xi_0)_t})dt - \beta\int_0^\theta (\rho_0, (\overline{\xi_0})_t)dt - \int_0^\theta (G, \xi_0)dt.
\end{aligned}$$

Applying the properties of $\overline{\xi}$, we have

$$\begin{aligned}
&\int_0^\theta \frac{1}{2}\frac{d}{dt}\|\xi_0\|^2 dt + \beta\int_0^\theta \|\xi_0\|dt - \int_0^\theta \frac{1}{2}\frac{d}{dt}A_{\alpha w}(\overline{\xi}, \overline{\xi})dt \\
=&\int_0^\theta ((\rho_0)_t, \xi_0)dt + \beta\int_0^\theta (\rho_0, \xi_0)dt - \int_0^\theta (G, \xi_0)dt.
\end{aligned} \tag{3.21}$$

By Lemma 2.1 and the boundedness of $\Psi(\boldsymbol{x})$ and Lipschitz continuity of $\sin(u)$, we derive

$$\begin{aligned}
\|\Psi(\boldsymbol{x})\sin(u) - \Psi(\boldsymbol{x})\sin(U)\|^2 \leq& C\|u - U\|^2 \\
\leq& C(\|u - Q_0u\| + \|Q_0u - U\|) \\
\leq& C\|\xi_0\|^2 + C\|\rho_0\|^2 + \|Q_0u - u\| \\
\leq& C\|\xi_0\|^2 + Ch^{2(k+1)}\|u\|_{k+1},
\end{aligned}$$

deduce that

$$\int_0^\theta (G, \xi_0)dt \leq Ch^{2(k+1)}\int_0^\theta \|u\|_{k+1}dt + \frac{\beta}{3}\int_0^\theta \|\xi_0\|^2 dt.$$

Now, we consider $\theta \in (0, T]$ satisfies $\|\xi(\theta)\| = \max_{0\leq t\leq T}\|\xi(t)\|$, according to (3.21), we have

$$\begin{aligned}
&\frac{1}{2}\|\xi_0(\theta)\|^2 + \beta\int_0^\theta \|\xi_0\|^2 + \frac{1}{2}A_{\alpha w}(\overline{\xi}(0), \overline{\xi}(0)) \\
\leq&\frac{1}{2}\|\xi_0(0)\|^2 + \int_0^\theta ((\rho_0)_t, \xi_0)dt + \beta\int_0^\theta (\rho_0, \xi_0)dt + \beta\int_0^\theta \|\xi_0\|^2 dt + Ch^{2(k+1)}\int_0^\theta \|u\|_{k+1}dt.
\end{aligned}$$

By applying 2.1 and Lemma 3.6 holds

$$\|\xi_0(0)\|^2 = \|U(0) - Q_hu(0)\|^2 + \|Q_hu(0) - R_hu(0)\|^2 \leq Ch^{2(k+1)}\|u(0)\|_{k+1}^2,$$

and

$$\begin{aligned}
\int_0^\theta ((\rho_0)_t, \xi_0)dt \leq& C\int_0^\theta \|(\rho_0)_t\|^2 dt + \frac{\beta}{3}\int_0^\theta \|\xi_0\|^2 dt \\
\leq& Ch^{2(k+1)}\int_0^\theta \|(u_0)_t\|^2 dt + \frac{\beta}{3}\int_0^\theta \|\xi_0\|^2 dt. \\
\int_0^\theta (\rho_0, \xi_0)dt \leq& C\int_0^\theta \|\rho_0\|^2 dt + \frac{\beta}{3}\int_0^\theta \|\xi_0\|^2 dt \\
\leq& Ch^{2(k+1)}\int_0^\theta \|u_0\|^2 dt + \frac{\beta}{3}\int_0^\theta \|\xi_0\|^2 dt.
\end{aligned}$$

Thus, we have

$$\|\xi_0(\theta)\|^2 \leq Ch^{2(k+1)}(\|(u_0)_t\|_{k+1}^2 + \|u_0\|_{k+1}^2 + \|u\|_{k+1}^2 + \|u(0)\|_{k+1}^2).$$

The conclusion is obtained.

4. Full–discrete scheme

In this section, we shall establish and analyze the fully–discrete SG equations (1.1)–(1.4). At first, introduce some notations and operators that will be used in this section.

For a given integer $N > 0$, let $\tau = T/N$ be the time step, $t^n = n\tau, n = 1, 2, \cdots, N$. For any function $\phi(x, y, t)$, set $\phi^n = \phi(x, y, t^n)$. For simplicity, define the following operators:

$$\begin{cases} \delta_t\phi^n = \dfrac{1}{2\tau}(\phi^{n+1} - \phi^{n-1}), \quad \delta_t^2\phi^n = \dfrac{1}{\tau^2}(\phi^{n+1} - 2\phi^n + \phi^{n-1}), \\ \overline{\phi^n} = \dfrac{1}{2}(\phi^{n+1} + \phi^{n-1}), \quad \phi^{n+\frac{1}{2}} = \dfrac{1}{2}(\phi^{n+1} + \phi^n), \quad \partial_t\phi^n = \dfrac{1}{\tau}(\phi^{n+1} - \phi^n). \end{cases}$$

Using the above notations, the fully discrete formulation of SG equation (1.1)–(1.4) is given as follows:

Find $U^{n+1} \in V_h, 1 \le n \le N-1$, such that

$$\begin{cases} (\delta_t^2 U_0^n, v_0) + \beta(\delta_t U_0^n, v_0) + A_{\alpha w}(\overline{U^n}, v_h) = (\Psi(\boldsymbol{x})\sin(U_0^n), v_0) + (f^n, v_0), \quad \forall v_h \in V_h, \\ U^0 = Q_h g_0, U^1 = Q_h g_0 + \tau Q_h g_1 + \dfrac{1}{2}\tau^2 Q_h u_{tt}(0), \end{cases} \tag{4.1}$$

where $Q_h u_{tt}(0)$ satisfy

$$(Q_h u_{tt}(0), v_0) = -\beta(Q_h u_t(0), v_0) - A_{\alpha w}(u(0), v_h) + (\Psi(\boldsymbol{x}, 0), v_0) + (f^0, v_0).$$

4.1. Stability of full-discrete scheme

Theorem 4.1. *Assume $U^n \in V_h^0$ is the solution of the problem of the fully discrete scheme (4.1), then it holds*

$$|||\, U^n|||^2 \le C, \tag{4.2}$$

where C is a constant independent of τ and h.

Proof. Notice $U^{n+1} - 2U^n + U^{n-1} = (U^{n+1} - U^n) - (U^n - U^{n-1})$, taking $v_h = (U^{n+1} - U^n) + (U^n - U^{n-1}) = U^{n+1} - U^{n-1}$ in the first equation of (4.1) we have

$$\begin{aligned} &(\delta_t^2 U_0^n, U_0^{n+1} - U_0^{n-1}) + \beta(\delta_t U_0^n, U_0^{n+1} - U_0^{n-1}) + A_{\alpha w}(\overline{U^n}, U^{n+1} - U^{n-1}) \\ =&(\Psi(\boldsymbol{x})\sin(U_0^n), U_0^{n+1} - U_0^{n-1}) + (f^n, U_0^{n+1} - U_0^{n-1}). \end{aligned}$$

By Cauchy–Schwarz and Young's inequalities, we have

$$\begin{aligned} &\frac{1}{\tau^2}\|U_0^{n+1} - U_0^n\|^2 - \frac{1}{\tau^2}\|U_0^n - U_0^{n-1}\|^2 + \frac{\beta}{2\tau}\|U_0^{n+1} - U_0^{n-1}\|^2 + |||U^{n+1}|||^2 - |||\, U^{n-1}|||^2 \\ =&(\Psi(\boldsymbol{x})\sin(U_0^n), U_0^{n+1} - U_0^{n-1}) + (f^n, U_0^{n+1} - U_0^{n-1}) \le C\tau(\|U_0^n\|^2 + \|f^n\|^2) + \frac{\beta}{2\tau}\|U_0^{n+1} - U_0^{n-1}\|^2. \end{aligned}$$

Summing up the inequality, and combined with the initial condition, we have

$$\frac{1}{\tau^2}\|U_0^{n+1} - U_0^n\|^2 + |||U^{n+1}|||^2 + |||\, U^n|||^2 \le \|g_1\|^2 + |||U^1|||^2 + |||\, U^0|||^2 + C\tau\sum_{1\le i\le n}(\|U_0^i\|^2 + \|f^i\|^2).$$

Finally, applying the discrete Gronwall's inequality, we have

$$|||U^n|||^2 \le \|g_1\|^2 + |||U^1|||^2 + |||\, U^0|||^2 + C\tau\sum_{1\le i\le n}\|f^i\|^2.$$

Through this derivation, the result is established.

4.2. Error estimates in the energy norm

Before analysis, we set $u^n - U^n = u^n - Q_h u^n + Q_h u^n - U^n := \eta_h^n + e_h^n$, the main result in this section presented in the following theorem.

Theorem 4.2. *Let u^n and $U^n \in V_h^0$ be the solutions of (1.1)–(1.4) and (4.1) in $t = n\tau$, respectively. If $u \in L^2(0,T;H^{k+1}(\Omega))$, $u_t \in L^2(0,T;H^{k+1}(\Omega))$, $u_{tt} \in L^2(0,T;H^{k+1}(\Omega))$, $u_{ttt} \in L^2(0,T;L^2(\Omega))$, $u_{tttt} \in L^2(0,T;L^2(\Omega))$, then there exists a constant $C > 0$ that is independent of h and τ and satisfies*

$$|||\, e_h^n \,||| \le C(h^k + \tau^2), \tag{4.3}$$

where C is independent of τ and h.

Proof. Add $\alpha S(Q_h u, v)$ to both sides of (3.2), then subtract the first equation of (4.1) from its average at t^{n-1} and t^{n+1}, and we get the error equation

$$\begin{aligned}
&(\overline{u_{tt}^n} - \delta_t^2 U_0^n, v_0) + \beta(\overline{u_t^n} - \delta_t U_0^n, v_0) + A_{\alpha w}(\overline{Q_h u^n} - \overline{U^n}, v_h)\\
=&l_1(\overline{u^n}, v) + l_2(\overline{u^n}, v) + l_3(\overline{u^n}, v) + \alpha S(\overline{Q_h u^n}, v)\\
&+ (\overline{f^n} - f^n, v_0) + (\Psi(\boldsymbol{x})(\frac{1}{2}(\sin(u^{n+1}) + \sin(u^{n-1})) - \sin(U_0^n)), v_0).
\end{aligned}$$

Since Q_h is a L^2 projection, we have

$$\begin{aligned}
&(\delta_t^2 Q_0 u^n - \delta_t^2 U_0^n, v_0) + \beta(\delta_t Q_0 u^n - \delta_t U_0^n, v_0) + A_{\alpha w}(\overline{Q_h u^n} - \overline{U^n}, v_h)\\
=&l_1(\overline{u^n}, v) + l_2(\overline{u^n}, v) + l_3(\overline{u^n}, v) + \alpha S(\overline{Q_h u^n}, v)\\
&+ (\overline{f^n} - f^n, v_0) + (\Psi(\boldsymbol{x})(\frac{1}{2}(\sin(u^{n+1}) + \sin(u^{n-1})) - \sin(U_0^n)), v_0)\\
&+ (\delta_t^2 u^n - u_{tt}^n, v_0) + (\delta_t u^n - u_t^n, v_0) + (u_{tt}^n - \frac{1}{2}\overline{u_{tt}^n}, v_0) + (u_t^n - \frac{1}{2}\overline{u_t^n}, v_0).
\end{aligned}$$

Taking $v_h = \delta_t e_h^n$, we get

$$\begin{aligned}
&\frac{1}{2\tau^3}(\|e_0^{n+1} - e_0^n\|^2 - \|e_0^n - e_0^{n-1}\|^2) + \beta\|\delta_t e_0^n\|^2 + \frac{1}{2\tau}(|||\, e_h^{n+1} \,|||^2 - |||\, e_h^{n-1} \,|||^2)\\
=&l_1(\overline{u^n}, \delta_t e^n) + l_2(\overline{u^n}, \delta_t e^n) + l_3(\overline{u^n}, \delta_t e^n) + \alpha S(\overline{Q_h u^n}, \delta_t e^n)\\
&+ (\overline{f^n} - f^n, \delta_t e_0^n) + (\Psi(\boldsymbol{x})(\frac{1}{2}(\sin(u^{n+1}) + \sin(u^{n-1})) - \sin(U_0^n)), \delta_t e_0^n)\\
&+ (\delta_t^2 u^n - u_{tt}^n, \delta_t e_0^n) + (\delta_t u^n - u_t^n, \delta_t e_0^n) + (u_{tt}^n - \frac{1}{2}\overline{u_{tt}^n}, \delta_t e_0^n) + (u_t^n - \frac{1}{2}\overline{u_t^n}, \delta_t e_0^n)\\
:=&\sum_{i=1}^{10} H_i.
\end{aligned}$$

By using Lemma 3.3, Lemma 2.4, and equivalence of norms, we derive

$$\begin{aligned}
|H_1| \le& Ch^k(\|u^{n+1}\|_{k+1} + \|u^{n-1}\|_{k+1})\, |||\, \delta_t e^n \,|||\\
\le& Ch^{2k}(\|u^{n+1}\|_{k+1}^2 + \|u^{n-1}\|_{k+1}^2) + \frac{1}{16\tau}(|||\, e^{n+1} \,|||^2 + |||\, e^{n-1} \,|||^2).
\end{aligned}$$

Then we can make a similar estimate for $\sum_{i=2}^{4} H_i$.

Next, we will estimate $H_5 \sim H_{10}$ one by one. By Cauchy–Schwarz inequality, Young's inequality, and Taylor expansion, we get

$$|H_5| = |(\overline{f^n} - f^n, \delta_t e_0^n)| \le \|\overline{f^n} - f^n\|\|\delta_t e_0^n\| \le C\tau^3 \int_{t^{n-1}}^{t^{n+1}} \|f_{tt}\|^2 dt + \frac{\beta}{6}\|\delta_t e_0^n\|^2,$$

$$\begin{aligned}
|H_6| =& |(\Psi(\boldsymbol{x})(\frac{1}{2}(\sin(u^{n+1}) + \sin(u^{n-1})) - \sin(U_0^n)), \delta_t e_0^n)| \\
\le& C|(\frac{1}{2}(\sin(u^{n+1}) + \sin(u^{n-1})) - \sin(u^n), \delta_t e_0^n)| + C|(\sin(u^n) - \sin(U_0^n), \delta_t e_0^n)| \\
\le& C\tau^2\|(\sin(u^n))_{tt}\|\|\delta_t e_0^n\| + C\|u^n - U^n\|\|\delta_t e_0^n\| \\
\le& C\tau^2\|(\sin(u^n))_{tt}\|\|\delta_t e_0^n\| + C(\|u^n - Q_0 u^n\| + \|Q_0 u^n - U_0^n\|)\|\delta_t e_0^n\| \\
\le& C\tau^3 \int_{t^{n-1}}^{t^{n+1}} \|(\sin(u))_{tt}\|^2 dt + Ch^{2(k+1)}\|u^n\|_{k+1} + C\|e_h^n\|^2 + \frac{\beta}{6}\|\delta_t e_0^n\|^2,
\end{aligned}$$

$$|H_7| = |(\delta_t^2 u^n - u_{tt}^n, \delta_t e_0^n)| \le C\tau^3 \int_{t^{n-1}}^{t^{n+1}} \|u_{tttt}\|^2 dt + \frac{\beta}{6}\|\delta_t e_0^n\|^2,$$

$$|H_8| = |(\delta_t u^n - u_t^n, \delta_t e_0^n)| \le C\tau^3 \int_{t^{n-1}}^{t^{n+1}} \|u_{ttt}\|^2 dt + \frac{\beta}{6}\|\delta_t e_0^n\|^2,$$

$$|H_9| = |(u_{tt}^n - \frac{1}{2}\overline{u_{tt}^n}, \delta_t e_0^n)| \le C\tau^2\|u_{tttt}^n\|\|\delta_t e_0^n\| \le C\tau^3 \int_{t^{n-1}}^{t^{n+1}} \|u_{tttt}\|^2 dt + \frac{\beta}{6}\|\delta_t e_0^n\|^2,$$

$$|H_{10}| = |(u_t^n - \frac{1}{2}\overline{u_t^n}, \delta_t e_0^n)| \le C\tau^2\|u_{ttt}^n\|\|\delta_t e_0^n\| \le C\tau^3 \int_{t^{n-1}}^{t^{n+1}} \|u_{ttt}\|^2 dt + \frac{\beta}{6}\|\delta_t e_0^n\|^2.$$

From all the inequalities above, we get

$$\begin{aligned}
&\frac{1}{2\tau^3}(\|e_0^{n+1} - e_0^n\|^2 - \|e_0^n - e_0^{n-1}\|^2) + \frac{1}{2\tau}(|||e_h^{n+1}|||^2 - |||e_h^{n-1}|||^2) \\
\le& C\tau^3(\int_{t^{n-1}}^{t^{n+1}} \|f_{tt}\|^2 dt + \int_{t^{n-1}}^{t^{n+1}} \|u_{tttt}\|^2 dt + \int_{t^{n-1}}^{t^{n+1}} \|u_{ttt}\|^2 dt) \\
&+ Ch^{2k}(\|u^{n+1}\|_{k+1}^2 + \|u^{n-1}\|_{k+1}^2) + C\|e_h^n\|^2 + \frac{1}{4\tau}(|||e^{n+1}|||^2 + |||e^{n-1}|||^2).
\end{aligned}$$

Summing up the inequality and multiplying by 2τ to get

$$\begin{aligned}
&\frac{1}{\tau^2}\|e_0^{n+1} - e_0^n\|^2 + |||e_h^{n+1}|||^2 + |||e_h^n|||^2 \\
\le& C\tau^4 \sum_{i=1}^{n}(\int_{t^{n-1}}^{t^{n+1}} \|f_{tt}\|^2 dt + \int_{t^{n-1}}^{t^{n+1}} \|u_{tttt}\|^2 dt + \int_{t^{n-1}}^{t^{n+1}} \|u_{ttt}\|^2 dt) \\
&+ Ch^{2k}\tau(\|u^{n+1}\|_{k+1}^2 + \|u^{n-1}\|_{k+1}^2) + C\tau\sum_{i=1}^{n}\|e_h^n\|^2 + C\sum_{i=1}^{n}|||e^i|||^2.
\end{aligned}$$

Finally, according to discrete Gromwall's inequality, we have

$$\begin{aligned}
&\frac{1}{\tau^2}\|e_0^{n+1}-e_0^n\|^2+|||e_h^{n+1}|||^2+|||e_h^n|||^2\\
\le&C\tau^4\sum_{i=1}^{n}\Big(\int_{t^{n-1}}^{t^{n+1}}\|f_{tt}\|^2dt+\int_{t^{n-1}}^{t^{n+1}}\|u_{tttt}\|^2dt+\int_{t^{n-1}}^{t^{n+1}}\|u_{ttt}\|^2dt\Big)\\
&+Ch^{2k}\tau(\|u^{n+1}\|_{k+1}^2+\|u^{n-1}\|_{k+1}^2).
\end{aligned}$$

Therefore, we conclude that

$$|||e_h^n||| \le C(h^k+\tau^2). \tag{4.4}$$

The proof is concluded here.

4.3. Error estimates in the L^2 norm of full-discrete scheme

Set

$$e_h^n = Q_hu^n-U^n = Q_hu^n-R_hu^n-(U^n-R_hu^n) := \rho_h^n-\xi_h^n,$$

we will prove the following theorem.

Theorem 4.3. *Let u^n and $U^n \in V_h^0$ be the solutions of (1.1)–(1.4) and (4.1) at $t = n\tau$, respectively. If $u \in L^2(0,T;H^{k+1}(\Omega))$, $u_t \in L^2(0,T;H^{k+1}(\Omega))$, $u_{tt} \in L^2(0,T;H^{k+1}(\Omega))$, $u_{ttt} \in L^2(0,T;L^2(\Omega))$, and $u_{tttt} \in L^2(0,T;L^2(\Omega))$, then there exists a constant $C > 0$, which is independent of h and τ, and satisfies*

$$\|\xi_0^{n+1}\| \le C(h^{k+1}+\tau^2), \tag{4.5}$$

where C is independent of τ and h.

Proof. For $v_h = \{v_0, v_b\} \in V_h^0$, we have

$$\begin{aligned}
&(\delta_t^2\xi_0^n, v_0)+\beta(\delta_t\xi_0^n, v_0)+A_{\alpha w}(\overline{\xi_h^n}, v_h)\\
=&(\delta_t^2U_0^n, v_0)+\beta(\delta_tU_0^n, v_0)+A_{\alpha w}(\overline{U_h^n}, v_h)-(\delta_t^2R_hu^n, v_0)-(\delta_tR_hu^n, v_0)-A_{\alpha w}(R_h\overline{u_h^n}, v_h)\\
=&(f^n, v_0)+(\Psi(\boldsymbol{x})\sin(U_0^n), v_0)-(\delta_t^2R_hu^n, v_0)-(\delta_tR_hu^n, v_0)-A_{\alpha w}(R_h\overline{u^n}, v_h)\\
=&(f^n, v_0)+(\Psi(\boldsymbol{x})\sin(U_0^n), v_0)-(\delta_t^2R_hu^n, v_0)-(\delta_tR_hu^n, v_0)+A_{\alpha w}(\nabla\cdot\nabla\overline{u^n}, v_h)\\
=&(f^n, v_0)+(\Psi(\boldsymbol{x})\sin(U_0^n), v_0)-(\delta_t^2R_hu^n, v_0)-(\delta_tR_hu^n, v_0)\\
&+((\overline{u_{tt}}+\beta\overline{u_t}-\Psi(\boldsymbol{x})\overline{\sin(u^n)}-\overline{f^n}), v_0)\\
=&(f^n-\overline{f^n}, v_0)+(\Psi(\boldsymbol{x})\sin(U_0^n)-\Psi(\boldsymbol{x})\overline{\sin(u^n)}, v_0)+(\delta_t^2\rho^n, v_0)+(\delta_t\rho^n, v_0)\\
&-(\delta_t^2(Q_hu^n-u^n), v_0)-(\delta_t(Q_hu^n-u^n), v_0)+(\overline{u_{tt}^n}-\delta_t^2u^n, v_0)+\beta(\overline{u_t^n}-\delta_tu^n, v_0)\\
:=&\sum_{i=1}^{5}T_i.
\end{aligned}$$

Where

$$T_1 = (f^n-\overline{f^n}, v_0), \tag{4.6}$$

$$T_2 = (\Psi(\boldsymbol{x})\sin(U^n)-\Psi(\boldsymbol{x})\overline{\sin(u^n)}, v_0), \tag{4.7}$$

$$T_3 =(\delta_t^2\rho^n, v_0) + (\delta_t\rho^n, v_0), \tag{4.8}$$

$$T_4 = -(\delta_t^2(Q_hu^n - u^n), v_0) - (\delta_t(Q_hu^n - u^n), v_0), \tag{4.9}$$

$$T_5 =(\overline{u_{tt}^n} - \delta_t^2u^n, v_0) + \beta(\overline{u_t^n} - \delta_tu^n, v_0). \tag{4.10}$$

Now, we will estimate $T_1 \sim T_5$ one by one.

By Cauchy–Schwarz inequality, Young's inequality, and Taylor's formula, we can bound $T_1 \sim T_2$ as follows:

$$\begin{aligned}
|T_1| =&|(f^n - \overline{f^n}, v_0)| \le C\tau^3\int_{t^{n-1}}^{t^{n+1}}\|f_{tt}\|^2dt + \frac{2\beta}{9}\|v_0\|^2.\\
|T_2| =&|(\Psi(\boldsymbol{x})\sin(U_0^n) - \Psi(\boldsymbol{x})\overline{\sin(u^n)}, v_0)|\\
\le&C|(\sin(U_0^n) - \sin(u^n) + \tau^2\sin(u)_{tt}, v_0)|\\
\le&C\|U^n - Q_0u^n\|\|v_0\| + Ch^{k+1}\|u\|_{k+1}\|v_0\| + C\tau^2\|\sin(u)_{tt}\|v_0\|\\
\le&Ch^{k+1}\|u\|_{k+1}\|v_0\| + C\tau^3\int_{t^{n-1}}^{t^{n+1}}\|\sin(u)_{tt}\|^2dt + \frac{2\beta}{9}\|v_0\|^2 + \|\xi_0^n\|\|v_0\|.
\end{aligned}$$

Then, applying Lemma 3.6, we have

$$|T_3| = |(\delta_t^2\rho^n, v_0) + (\delta_t\rho^n, v_0)| \le Ch^{k+1}\|\delta_t^2u^n\|_{k+1}\|v_0\| + Ch^{k+1}\|\delta_tu^n\|_{k+1}\|v_0\|.$$

Next, from Lemma 2.1 that

$$|T_4| = |(\delta_t^2(Q_hu^n - u^n), v_0) + (\delta_t(Q_hu^n - u^n), v_0)| \le Ch^{k+1}\|\delta_t^2u^n\|_{k+1}\|v_0\| + Ch^{k+1}\|\delta_tu^n\|_{k+1}\|v_0\|.$$

Finally, similar to the proof of $T_1 \sim T_2$, we get

$$|T_5| = |(\overline{u_{tt}^n} - \delta_t^2u^n, v_0) + \beta(\overline{u_t^n} - \delta_tu^n, v_0)| \le C\tau^3\int_{t^{n-1}}^{t^{n+1}}\|u_{tttt}\|^2dt + C\tau^3\int_{t^{n-1}}^{t^{n+1}}\|u_{ttt}\|^2dt + \frac{2\beta}{9}\|v_0\|^2.$$

Hence, combining the above estimates $T_1 \sim T_5$, we have

$$\begin{aligned}
&(\delta_t^2\xi_0^n, v_0) + \beta(\delta_t\xi_0^n, v_0) + A_{\alpha w}(\overline{\xi^n}, v_h)\\
\le&C\tau^3\int_{t^{n-1}}^{t^{n+1}}\|f_{tt}\|^2dt + C\tau^3\int_{t^{n-1}}^{t^{n+1}}\|\sin(u)_{tt}\|^2dt + C\tau^3\int_{t^{n-1}}^{t^{n+1}}\|u_{tttt}\|^2dt + C\tau^3\int_{t^{n-1}}^{t^{n+1}}\|u_{ttt}\|^2dt\\
&+ Ch^{k+1}(\|\delta_t^2u^n\|_{k+1} + \|u\|_{k+1} + \|\delta_tu^n\|_{k+1})\|v_0\| + \|\xi_0^n\|\|v_0\| + \frac{2\beta}{3}\|v_0\|^2.
\end{aligned} \tag{4.11}$$

Taking $v = \delta_t\xi_0^n$ in equation (4.11) to obtain

$$\begin{aligned}
&\frac{1}{2\tau}\Big(\frac{\|\xi_0^{n+1} - \xi_0^n\|^2}{\tau^2} - \frac{\|\xi_0^n - \xi_0^{n-1}\|^2}{\tau^2}\Big) + \beta\|\delta_t\xi_0^n\|^2 + \frac{1}{2\tau}(|||\xi^{n+1}|||^2 - |||\xi^{n-1}|||^2)\\
\le&C\tau^3\int_{t^{n-1}}^{t^{n+1}}\|f_{tt}\|^2dt + C\tau^3\int_{t^{n-1}}^{t^{n+1}}\|\sin(u)_{tt}\|^2dt + C\tau^3\int_{t^{n-1}}^{t^{n+1}}\|u_{tttt}\|^2dt + C\tau^3\int_{t^{n-1}}^{t^{n+1}}\|u_{ttt}\|^2dt\\
&+ Ch^{k+1}(\|\delta_t^2u^n\|_{k+1} + \|u\|_{k+1} + \|\delta_tu^n\|_{k+1})\|\delta_t\xi_0^n\| + \|\xi_0^n\|\|\delta_t\xi_0^n\| + \frac{2\beta}{3}\|\delta_t\xi_0^n\|^2.
\end{aligned}$$

Therefore, multiplying τ on both sides of the above and applying Young's inequality, we get

$$\begin{aligned}
&(\frac{\|\xi_0^{n+1}-\xi_0^n\|^2}{\tau^2}-\frac{\|\xi_0^n-\xi_0^{n-1}\|^2}{\tau^2})+2\beta\tau\|\delta_t\xi_0^n\|^2+(|||\xi^{n+1}|||^2-|||\xi^{n-1}|||^2)\\
\leq& C\tau^4\int_{t^{n-1}}^{t^{n+1}}\|f_{tt}\|^2dt+C\tau^4\int_{t^{n-1}}^{t^{n+1}}\|\sin(u)_{tt}\|^2dt+C\tau^4\int_{t^{n-1}}^{t^{n+1}}\|u_{tttt}\|^2dt+C\tau^4\int_{t^{n-1}}^{t^{n+1}}\|u_{ttt}\|^2dt\\
&+Ch^{2(k+1)}(\|\delta_t^2u^n\|_{k+1}^2+\|u\|_{k+1}^2+\|\delta_tu^n\|_{k+1}^2)+C\tau\|\xi_0^n\|^2+2\beta\tau\|\delta_t\xi_0^n\|^2.
\end{aligned}$$

Now, applying discrete Gronwall's inequality and summing over 1 to n, we arrive at

$$\begin{aligned}
&(\|\partial\xi_0^n\|^2-\|\partial\xi_0^0\|^2)+(|||\xi^{n+1}|||^2+|||\xi^n|||^2-|||\xi^1|||^2-|||\xi^0|||^2)\\
\leq& C\tau^4(\|f_{tt}\|^2_{L^2(L^2(\Omega))}+\|\sin(u)_{tt}\|^2_{L^2(L^2(\Omega))}+\|u_{tttt}\|^2_{L^2(L^2(\Omega))}+\|u_{tttt}\|^2_{L^2(L^2(\Omega))})\\
&+Ch^{2(k+1)}(\|u\|^2_{L^\infty(H^{k+1}(\Omega))}+\|u_t\|^2_{L^\infty(H^{k+1}(\Omega))}+\|u_{tt}\|^2_{L^\infty(H^{k+1}(\Omega))})+C\tau\sum_{i=1}^{n-1}\|\xi_0^i\|^2.
\end{aligned}\tag{4.12}$$

Since, $\xi^n=\xi^{n-\frac{1}{2}}+\frac{\tau}{2}\partial_t\xi^{n-1}$

$$\|\xi^n\|^2\leq\|\xi^{n-\frac{1}{2}}\|^2+\frac{\tau^2}{4}\|\partial_t\xi^{n-\frac{1}{2}}\|^2\leq\|\xi^{n-\frac{1}{2}}\|^2+\|\partial_t\xi^{n-1}\|^2.\tag{4.13}$$

By Eq (4.13) and adding $\|\xi_0^{n-\frac{1}{2}}\|^2$ to both sides of (4.12), we have

$$\begin{aligned}
\|\xi_0^n\|^2+|||\xi^n|||^2+|||\xi^{n-1}|||^2\leq&2\|\partial_t\xi_0^0\|^2+|||\xi^1|||^2+|||\xi^0|||^2+\|\xi_0^{n-1}\|^2+C\tau\sum_{i=1}^{n-1}\|\xi_0^i\|^2\\
&+C\tau^4(\|f_{tt}\|^2_{L^2(L^2(\Omega))}+\|\sin(u)_{tt}\|^2_{L^2(L^2(\Omega))}+\|u_{tttt}\|^2_{L^2(L^2(\Omega))}+\|u_{tttt}\|^2_{L^2(L^2(\Omega))})\\
&+Ch^{2(k+1)}(\|u\|^2_{L^\infty(H^{k+1}(\Omega))}+\|u_t\|^2_{L^\infty(H^{k+1}(\Omega))}+\|u_{tt}\|^2_{L^\infty(H^{k+1}(\Omega))}).
\end{aligned}$$

Again, applying discrete Gronwall's inequality and notice $\xi^0=0$, $\xi^1=o(\tau^2)$, it yields

$$\begin{aligned}
\|\xi_0^n\|^2\leq&C\tau^4(\|f_{tt}\|^2_{L^2(L^2(\Omega))}+\|\sin(u)_{tt}\|^2_{L^2(L^2(\Omega))}+\|u_{tttt}\|^2_{L^2(L^2(\Omega))}+\|u_{tttt}\|^2_{L^2(L^2(\Omega))})+o(\tau^4)\\
&+Ch^{2(k+1)}(\|u\|^2_{L^\infty(H^{k+1}(\Omega))}+\|u_t\|^2_{L^\infty(H^{k+1}(\Omega))}+\|u_{tt}\|^2_{L^\infty(H^{k+1}(\Omega))}).
\end{aligned}$$

We have thus proved the result.

5. UWG-POD scheme

First, calculate the previous L numerical solutions $U^i=\{U_0^i,U_b^i\}$ of problem (1.1) by the SFWG method.Then constructed snapshot matrix A.The matrix $A=(A_{ij})_{L\times L}$ is positive semi-definite and is defined as:

$$A_{ij}=\frac{1}{L}\sum_{T\in\mathcal{T}_h}(U_0^i,U_0^j)\tag{5.1}$$

where $i,j=1,2,\cdots,L$. Snapshot matrix A implies the characteristic information of previous L numerical solutions. POD bases can be constructed as follow.

Let $\lambda_1 \geq \lambda_2 \geq \cdots \geq \lambda_l$ denote the eigenvalues of A, $\boldsymbol{v_1}, \boldsymbol{v_2}, \cdots, \boldsymbol{v_l}$ represent the corresponding standard orthogonal eigenvectors. Then the POD bases with rank $d \leq l$ are generated by:

$$\psi_{i0} = \frac{1}{\sqrt{L\lambda_i}} \sum_{j=1}^{L} ((\boldsymbol{v_i})_j U_0^i), \quad \psi_{ib} = \frac{1}{\sqrt{L\lambda_i}} \sum_{j=1}^{L} ((\boldsymbol{v_i})_j U_b^i). \tag{5.2}$$

Where $i = 1, 2, \cdots, d$, and $(\boldsymbol{v_i})_j$ denotes the j th component of the standard orthogonal eigenvector $\boldsymbol{v_i}$. Then we can span the reduced-order space V_d by POD basis. The UWG-POD scheme of problem (1.1) is as follows.

Find $U_d^n = \{U_{d0}^n, U_{db}^n\}$, $n = L+1, L+2, \cdots, N$, for all $v_d \in V_d$ such that

$$(\delta_t^2 U_{d0}^n, v_{d0}) + \beta(\delta_t U_{d0}^n, v_{d0}) + A_{\alpha w}(\overline{U_d^n}, v_d) = (\Psi(\boldsymbol{x}) \sin(U_{d0}^n), v_{d0}) + (f^n, v_{d0}). \tag{5.3}$$

Algorithm 5.1 UWG-POD algorithm

Step 1: Use the UWG to obtain the snapshot matrix $u_h^n = \{u_0^n, u_b^n\}$, $n = 1, 2, \ldots, L$.

Step 2: Assemble the snapshot matrix $A = (A_{ij})_{L\times L}$ by (5.1).

Step 3: Calculate the eigenvalues $\lambda_1, \lambda_2, \ldots, \lambda_L$ of A and their corresponding orthonormal eigenvectors $v_i = (v_{i1}, v_{i2}, \ldots, v_{iL})'$, $1 \leq i \leq l$.

Step 4: Establish criteria to determine the quantity of POD basis d.

Step 5: Calculate the POD basis $\psi_i = \{\psi_{i0}, \psi_{ib}\}$ by (5.2) and denote the POD space by $V_d = \text{span}\{\psi_1, \psi_2, \ldots, \psi_d\}$.

Step 6: Solve the reduced-order model (5.3) and obtain the reduced-order solution $u_d^n \in V_d$.

Step 7: If $\|u_d^{n+1,0} - u_d^{n,0}\| \leq \|u_d^{n,0} - u_d^{n-1,0}\|$, $n = 1, 2, \ldots, N-1$, then the reduced-order model solutions satisfy the desirable accuracy.

Else extract the new snapshots u_{j+L}^n, $j = 1, 2, \ldots, L$, and return to Step 2.

6. Numerical examples

In this section, we present two numerical experiments to confirm the convergence rates and efficiency of our proposed methods. The WG component is based on the open-source program developed by Qilong Zhai's team [40] from Jilin University. We have implemented these numerical tests on a system running Windows 11, with an Intel(R) Core(TM) i7-8565U CPU @ 1.80GHz.

6.1. Example 1

In this example, we perform calculations under the domain $\Omega = [0, 1] \times [0, 1]$ and $T = 1$. For simplicity, take $\Psi(x, y) = 1$ and $\beta = 1$. The analytical solution of (1.1)–(1.4) is given by:

$$u = \frac{1}{\sin(1/(t+1))} x^2(x-1)\sin(\pi y)(1+3t^2).$$

Then the source term f and initial value $g_0(x, y)$, $g_1(x, y)$ can be directly obtained.

Table 6.1. Error profiles and convergence order of scheme (4.1) with $k = 1$ and $\tau = \frac{1}{20}h$.

	$\alpha = 0,\ j = 3$				$\alpha = 1,\ j = 0$			
h	$\|\|\|e_h\|\|\|$	Order	$\|e_h\|$	Order	$\|\|\|e_h\|\|\|$	Order	$\|e_h\|$	Order
1/16	3.0583E-01	–	3.0638E-03	–	3.7842E-01	–	1.3459E-02	–
1/32	1.5233E-01	1.0055	7.6550E-04	2.0008	1.8764E-01	1.0120	3.3662E-03	1.9994
1/64	7.7287E-02	0.9789	1.9200E-04	1.9953	9.3374E-02	1.0069	8.3957E-04	2.0034
1/128	3.7605E-02	1.0393	4.7604E-05	2.0120	4.6717E-02	0.9991	2.0985E-04	2.0003

As shown in Table 6.1, the proposed method can achieve ideal approximation accuracy and expected convergence orders both with and without stabilizers.

Table 6.2. Error profiles and convergence order of scheme (5.3) with $k = 1$ and $\tau = \frac{1}{20}h$.

	$\alpha = 0,\ j = 3,\ L = 20,\ d = 5$				$\alpha = 1,\ j = 0,\ L = 20,\ d = 5$			
h	$\|\|\|e_h\|\|\|$	Order	$\|e_h\|$	Order	$\|\|\|e_h\|\|\|$	Order	$\|e_h\|$	Order
1/16	3.4303E-01	-	3.0747E-03	-	4.4490E-01	-	1.3794E-02	-
1/32	1.7622E-01	0.9609	7.7341E-04	1.9911	2.1106E-01	0.9663	3.5949E-03	1.9400
1/64	8.3366E-02	1.0798	1.9127E-04	2.0155	1.0374E-01	1.0247	9.2909E-04	1.9521
1/128	4.2213E-02	0.9817	4.7847E-05	1.9991	5.2493E-02	0.9828	2.3592E-04	1.9775

By comparing Table 6.1 with Table 6.2, it can be seen that we performed reduced-order computations on the model, the algorithm still maintained the original accuracy and convergence order, which strongly demonstrates the effectiveness of the reduced-order algorithm.

Table 6.3. Comparison of computation time.

h	$\alpha = 0,\ j = 3,\ k = 1,\ \tau = \frac{1}{20}h$		$\alpha = 1,\ j = 0,\ k = 1,\ \tau = \frac{1}{20}h$	
	WG	WG-POD	WG	WG-POD
1/16	6.4s	1.8s	4.4s	0.6s
1/32	47.9s	10.7s	33.1s	5.0s
1/64	720.8s	45.9s	699.0s	36.1s
1/128	5954.6s	284.8s	4229.1s	267.4s

The computational efficiency of the reduced-order model is clearly demonstrated in Table 6.3. For instance, when the mesh size parameter $h = 1/128$, the full-order model requires more than ten times the computational time of the reduced-order model. This clearly indicates that the advantages of the reduced-order algorithm become increasingly prominent as the problem scale expands.

Figure 6.1 intuitively shows the convergence of computational formats (4.1) and (5.3) and the advantage of format (5.3) in efficiency. Though the time bar chart's height is less obvious due to the log-scale y-axis, the actual values differ by about tenfold.

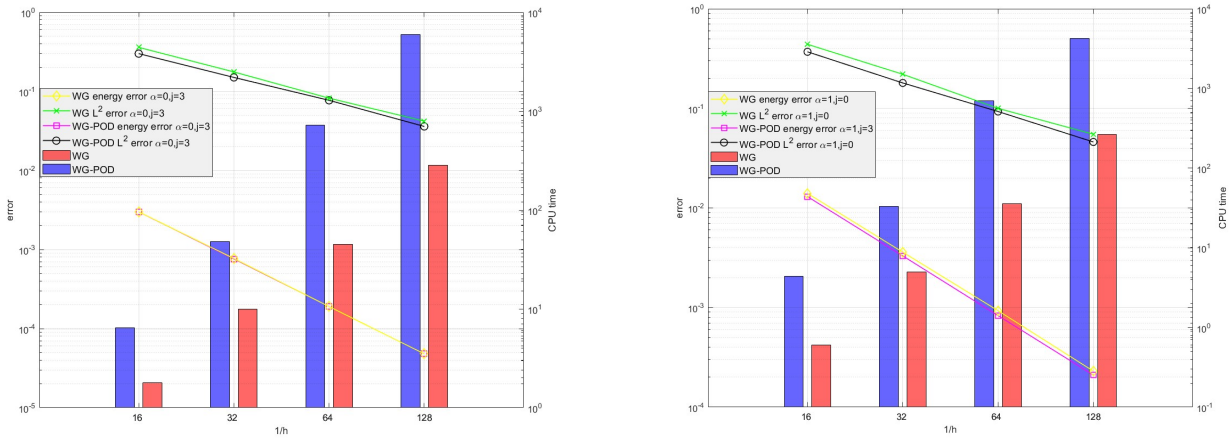

Figure 6.1. The log-log convergence plots and bar charts for CPU time vs. mesh size of WG and WG-POD (left), SFWG and SFWG-POD (right).

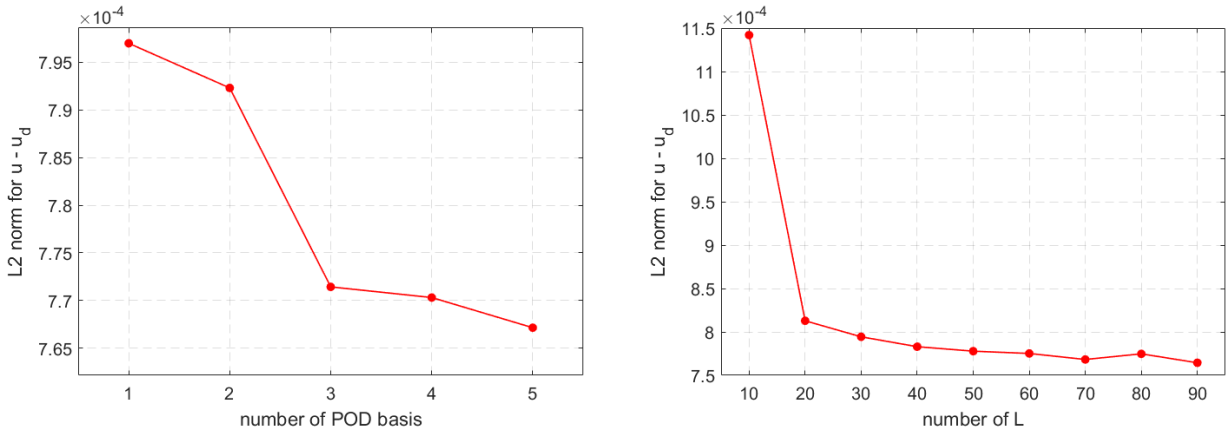

Figure 6.2. The relationship between the error and the number of POD basis function d (left), and number of sampling L (right) with $h = 1/32$, $\tau = 1/3200$.

Figure 6.2 illustrates the effects of two key parameters in the WG-POD method on error behavior. The left sub-figure demonstrates that the error decreases as the number of POD basis functions increases, yet only a small number of basis functions are necessary to achieve sufficient accuracy. The right sub-figure reveals that the error decreases suddenly as L increases and then becomes stable.

6.2. Example 2: Superposition of two line solitons

In this example, we consider the problem of superposition of two line solitons.

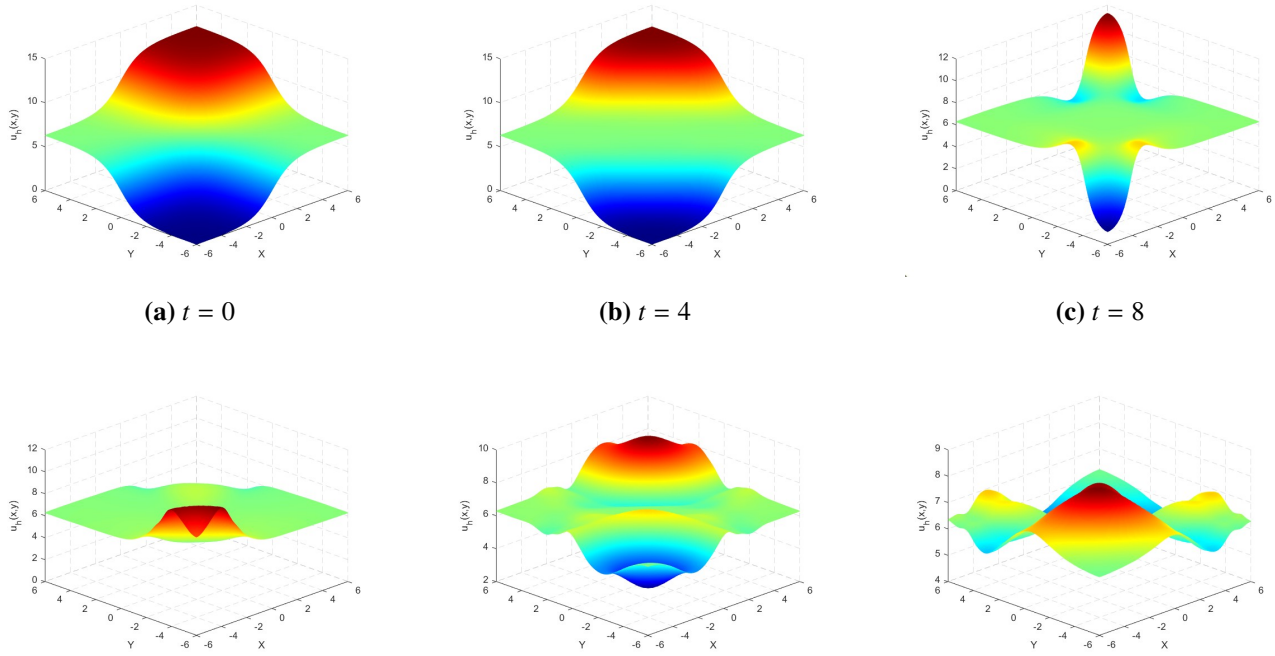

(a) $t = 0$ **(b)** $t = 4$ **(c)** $t = 8$

(d) $t = 12$ **(e)** $t = 16$ **(f)** $t = 20$

Figure 6.3. Snapshots at different time steps ($\beta = 0$).

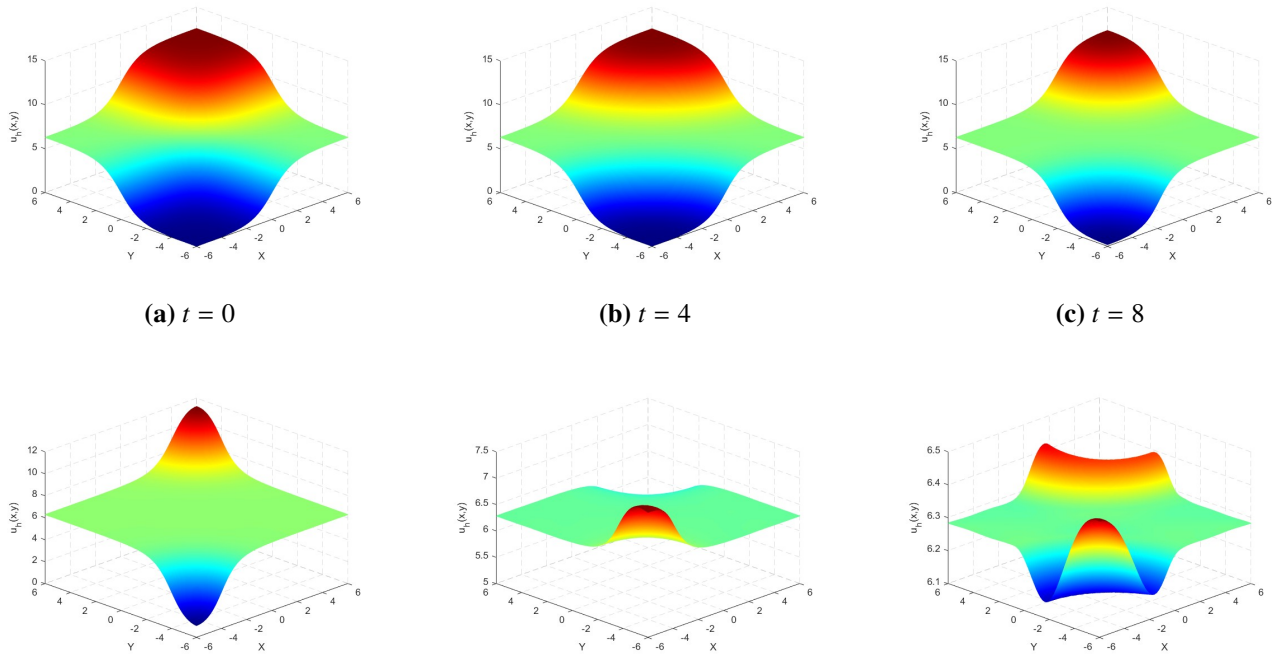

(a) $t = 0$ **(b)** $t = 4$ **(c)** $t = 8$

(d) $t = 12$ **(e)** $t = 16$ **(f)** $t = 20$

Figure 6.4. Snapshots at different time steps ($\beta = 0.5$).

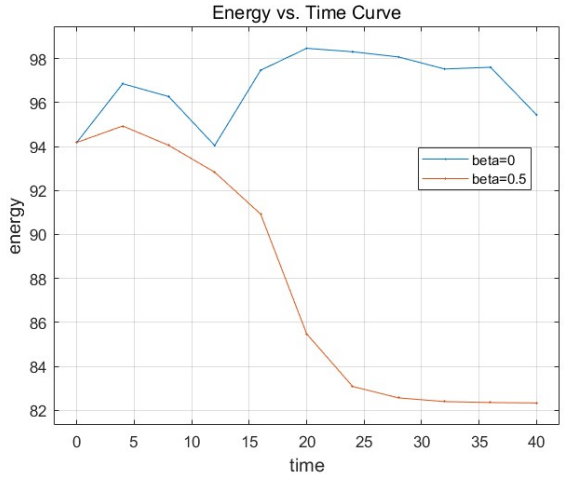

Figure 6.5. Energy decay curves for the superposition of two line solitons example.

In applied physics, phenomena such as the propagation of magnetic flux quanta in long Josephson junctions and the dynamics of crystal dislocations are effectively described by the sine-Gordon equation. Of particular theoretical and practical significance is the superposition of two line solitons, which characterizes the nonlinear interaction of extended solitary waves. This process highlights the intrinsic stability and particle-like behavior of solitons, offering valuable insights into complex wave dynamics observed in real-world systems.

This problem does not have a smooth solution, and we only know $f = 0$ and $\Psi(x, y) = 1$, along with the following initial conditions:

$$\begin{aligned} u(x, y, 0) =& 4\tan^{-1}(\exp(x)) + 4\tan^{-1}(\exp(y)), \\ u_t(x, y, 0) =& 0, \quad -6 \le x, y \le 6. \end{aligned}$$

We will examine the cases $\beta = 0$ and $\beta = 0.5$ separately to intuitively observe the role of the damping term when two orthogonal line solitons intersect.

The numerical results are given at $t = 0, 4, \cdots, 20$. We computed this example with $h = 1/64$, $\tau = 0.01$, and $k = 1$.

At $t = 0$, both solitons share the same initial state, and as time progresses, the two line solitons propagate toward each other. By comparing Figures 6.3 and 6.4, the delaying effect of the damping term on the propagation of the line solitons becomes evident, along with observable energy dissipation. Moreover, these effects grow increasingly pronounced over time; this conclusion agrees with [41] and [42]. Figure 6.5 allows us to more intuitively see the curve of the energy $E(u)$ changing with time. Here, we define $E(u) = \frac{1}{2}\int_\Omega u_{0_t}^2 + \nabla_w u^2 + 2(1 - \cos(u_0))dxdy$. Due to parameter selection and discrete computation reasons, there are some slight fluctuations in the energy curve. However, it can be clearly seen that the energy change curve when $\beta = 0.5$, compared with the case when $\beta = 0$, shows a downward trend.

7. Conclusions and remark

This work presents and analyzes an effective fully discrete explicit scheme for the damped sine-Gordon equation. The scheme is based on the WG method in spatial direction, where $\alpha = 0$ is for

SFWG and $\alpha = 1$ is for the classical WG method. In the temporal direction, we use the second-order explicit differentiation formula. The optimal order of convergence in the energy norm and the L^2 norm are derived. Furthermore, in order to improve the computational efficiency, we develop a reduced-order algorithm by combining the POD technique with the UWG method. The experimental results verify the correctness of our theory. Especially when the mesh size parameter $h = 1/128$, the full-order model requires more than 10 times the computational time of the reduced-order model in Example 1. In the future, we will discuss the superconvergence of the UWG method for the SG equation (1.1)–(1.4) by decomposing the error via temporal, spatial, and space–time hybrid projections, deriving the leading error terms and higher–order terms, and thereby identifying natural space–time superconvergent points. Then we approximate the leading error terms and construct space–time postprocessed WG solutions and corresponding a posteriori error estimators and the theoretical analysis of the time complexity of the proposed scheme.

Use of AI tools declaration

The authors declare they have not used Artificial Intelligence (AI) tools in the creation of this article.

Acknowledgments

This research was supported by the Sichuan Science and Technology Program (2022JDTD0019) and the Natural Science Foundation of Sichuan Province (No. 2025ZNSFSC0070).

Conflict of interest

The authors declare there is no conflicts of interest.

References

1. C. L. Terng, A higher dimension generalization of the sine-Gordon equation and its soliton theory, *Ann. Math.*, **111** (1980), 491–510. https://doi.org/10.2307/1971106
2. S. Watanabe, H. S. van der Zant, S. H. Strogatz, T. P. Orlando, Dynamics of circular arrays of Josephson junctions and the discrete sine-Gordon equation, *Physica D*, **97** (1996), 429–470. https://doi.org/10.1016/0167-2789(96)00083-8
3. O. Nikan, Z. Avazzadeh, M. Rasoulizadeh, Soliton solutions of the nonlinear sine-Gordon model with Neumann boundary conditions arising in crystal dislocation theory, *Nonlinear Dyn.*, **106** (2021), 783–813. https://doi.org/10.1007/s11071-021-06822-4
4. P. Grinevich, S. Novikov, Topological charge of the real periodic finite-gap sine-Gordon solutions, *Commun. Pure Appl. Math.*, **56** (2003), 956–978. https://doi.org/10.1002/cpa.10081
5. J. D. Gibbon, I. N. James, I. M. Moroz, The sine-Gordon equation as a model for a rapidly rotating baroclinic fluid, *Phys. Scr.*, **20** (1979), 402. https://doi.org/10.1088/0031-8949/20/3-4/015
6. M. H. Uddin, U. Zaman, M. A. Arefin, M. A. Akbar, Nonlinear dispersive wave propagation pattern in optical fiber system, *Chaos, Solitons Fractals*, **164** (2022), 112596. https://doi.org/10.1016/j.chaos.2022.112596

7. S. Duan, Y. Ma, W. Zhang, Conformal-type energy estimates on hyperboloids and the wave-Klein-Gordon model of self-gravitating massive fields, *Commun. Anal. Mech.*, **15** (2023), 111–131. https://doi.org/10.3934/cam.2023007
8. F. Mirzaee, S. Rezaei, N. Samadyar, Numerical solution of two-dimensional stochastic time-fractional sine-Gordon equation on non-rectangular domains using finite difference and meshfree methods, *Eng. Anal. Boundary Elem.*, **127** (2021), 53–63. https://doi.org/10.1016/j.enganabound.2021.03.009
9. Y. Yang, C. Wen, Y. Liu, H. Li, J. Wang, Optimal time two-mesh mixed finite element method for a nonlinear fractional hyperbolic wave model, *Commun. Anal. Mech.*, **16** (2024), 24–52. https://doi.org/10.3934/cam.2024002
10. R. Jiwari, Barycentric rational interpolation and local radial basis functions based numerical algorithms for multidimensional sine-Gordon equation, *Numer. Methods Partial Differ. Equations*, **37** (2021), 1965–1992. https://doi.org/10.1002/num.22636
11. M. Ratas, A. Salupere, J. Majak, Solving nonlinear PDEs using the higher order Haar wavelet method on nonuniform and adaptive grids, *Math. Model. Anal.*, **26** (2021), 147–169. https://doi.org/10.3846/mma.2021.12920
12. H. Zhang, X. Qian, J. Xia, S. Song, Unconditionally maximum-principle-preserving parametric integrating factor two-step Runge-Kutta schemes for parabolic sine-Gordon equations, *CSIAM Trans. Appl. Math.*, **4** (2023), 177–224. https://doi.org/10.4208/csiam-am.SO-2022-0019
13. J. Y. Wang, Q. A. Huang, A family of effective structure-preserving schemes with second-order accuracy for the undamped sine-Gordon equation, *Comput. Math. Appl.*, **90** (2021), 38–45. https://doi.org/10.1016/j.camwa.2021.03.009
14. A. Al-Taweel, J. Alkhalissi, X. Wang, The Crank-Nicolson weak Galerkin finite element methods for the sine-Gordon equation, *Appl. Numer. Math.*, **212** (2025), 77–91. https://doi.org/10.1016/j.apnum.2025.01.016
15. J. Wang, X. Ye, A weak Galerkin finite element method for second-order elliptic problems, *J. Comput. Appl. Math.*, **241** (2013), 103–115. https://doi.org/10.1016/j.cam.2012.10.003
16. J. Wang, X. Ye, A weak Galerkin mixed finite element method for second order elliptic problems, *Math. Comput.*, **83** (2014), 2101–2126. https://doi.org/10.1090/S0025-5718-2014-02852-4
17. L. Zhang, M. Feng, J. Zhang, A globally divergence-free weak Galerkin method for Brinkman equations, *Appl. Numer. Math.*, **137** (2019), 213–229. https://doi.org/10.1016/j.apnum.2018.11.002
18. X. Li, A weak Galerkin meshless method for incompressible Navier-Stokes equations, *J. Comput. Appl. Math.*, **445** (2024), 115823. https://doi.org/10.1016/j.cam.2024.115823
19. D. Li, C. Wang, J. Wang, Generalized weak Galerkin finite element methods for biharmonic equations, *J. Comput. Appl. Math.*, **434** (2023), 115353. https://doi.org/10.1016/j.cam.2023.115353
20. F. Huo, R. Wang, Y. Wang, R. Zhang, A locking-free weak Galerkin finite element method for linear elasticity problems, *Comput. Math. Appl.*, **160** (2024), 181–190. https://doi.org/10.1016/j.camwa.2024.02.032

21. W. Li, F. Gao, J. Cui, A weak Galerkin finite element method for nonlinear convection-diffusion equation, *Appl. Math. Comput.*, **461** (2024), 128315. https://doi.org/10.1016/j.amc.2023.128315

22. J. Zhang, X. Liu, Uniform convergence of a weak Galerkin finite element method on Shishkin mesh for singularly perturbed convection-diffusion problems in 2D, *Appl. Math. Comput.*, **432** (2022), 127346. https://doi.org/10.1016/j.amc.2022.127346

23. P. Jana, N. Kumar, B. Deka, Weak Galerkin finite element methods for semilinear Klein-Gordon equation on polygonal meshes, *Comput. Appl. Math.*, **43** (2024), 218. https://doi.org/10.1007/s40314-024-02745-z

24. X. Ye, S. Zhang, A stabilizer-free weak Galerkin finite element method on polytopal meshes, *J. Comput. Appl. Math.*, **371** (2020), 112699. https://doi.org/10.1016/j.cam.2019.112699

25. X. Ye, S. Zhang, A stabilizer free weak Galerkin finite element method on polytopal mesh: Part II, *J. Comput. Appl. Math.*, **394** (2021), 113525. https://doi.org/10.1016/j.cam.2021.113525

26. X. Ye, S. Zhang, A stabilizer free weak Galerkin finite element method on polytopal mesh: Part III, *J. Comput. Appl. Math.*, **394** (2021), 113538. https://doi.org/10.1016/j.cam.2021.113538

27. Y. Feng, Y. Liu, R. Wang, S. Zhang, A stabilizer-free weak Galerkin finite element method for the Stokes equations, *Adv. Appl. Math. Mech.*, **14** (2022), 181–201. https://doi.org/10.4208/aamm.OA-2020-0325

28. S. Wang, J. Ma, N. Du, A stabilizer-free weak Galerkin finite element method for an optimal control problem of a time fractional diffusion equation, *Math. Comput. Simul.*, **231** (2025), 99–118. https://doi.org/10.1016/j.matcom.2024.11.019

29. X. Wang, X. Ye, S. Zhang, Weak Galerkin finite element methods with or without stabilizers, *Numer. Algorithms*, **88** (2021), 1361–1381. https://doi.org/10.1007/s11075-021-01079-9

30. K. Kunisch, S. Volkwein, Galerkin proper orthogonal decomposition methods for parabolic problems, *Numer. Math.*, **90** (2001), 117–148. https://doi.org/10.1007/s002110100282

31. K. Kunisch, S. Volkwein, Galerkin proper orthogonal decomposition methods for a general equation in fluid dynamics, *SIAM J. Numer. Anal.*, **40** (2002), 492–515. https://doi.org/10.1137/S0036142900382612

32. J. R. Singler, New POD error expressions, error bounds, and asymptotic results for reduced order models of parabolic PDEs, *SIAM. J. Numer. Anal.*, **52** (2014), 852–876. https://doi.org/10.1137/120886947

33. J. Shen, J. R. Singler, Y. Zhang, HDG-POD reduced order model of the heat equation, *J. Comput. Appl. Math.*, **362** (2019), 663–679. https://doi.org/10.1016/j.cam.2018.09.031

34. K. Li, T. Huang, L. Li, S. Lanteri, L. Xu, B. Li, A reduced-order discontinuous Galerkin method based on POD for electromagnetic simulation, *IEEE Trans. Antennas Propag.*, **66** (2017), 242–254. https://doi.org/10.1109/TAP.2017.2768562

35. S. He, H. Li, Y. Liu, A POD based extrapolation DG time stepping space-time FE method for parabolic problems, *J. Math. Anal. Appl.*, **539** (2024), 128501. https://doi.org/10.1016/j.jmaa.2024.128501

36. L. Wang, M. Feng, The simplified weak Galerkin method with θ scheme and its reduced-order model for the elastodynamic problem on polygonal mesh, *Comput. Math. Appl.*, **178** (2025), 19–46. https://doi.org/10.1016/j.camwa.2024.11.023

37. W. Han, L. He, F. Wang, Optimal order error estimates for discontinuous Galerkin methods for the wave equation, *J. Sci. Comput.*, **78** (2019), 121–144. https://doi.org/10.1007/s10915-018-0755-1

38. H. Wang, D. Xu, J. Zhou, J. Guo, Weak Galerkin finite element method for a class of time fractional generalized Burgers' equation, *Numer. Methods Partial Differ. Equations*, **37** (2021), 732–749. https://doi.org/10.1002/num.22549

39. L. Wang, Y. Tan, M. Feng, The two-grid hybrid high-order method for the nonlinear strongly damped wave equation on polygonal mesh and its reduced-order model, *Appl. Numer. Math.*, **210** (2025), 1–24. https://doi.org/10.1016/j.apnum.2024.12.006

40. Q. Zhai, R. Wang, L. Mu, Implementation of weak Galerkin finite element methods, 2016. Available from: https://github.com/MollyRaver/WGFEMPoisson.

41. M. Dehghan, D. Mirzaei, The dual reciprocity boundary element method (DRBEM) for two-dimensional sine-Gordon equation, *Comput. Methods Appl. Mech. Eng.*, **197** (2008), 476–486. https://doi.org/10.1016/j.cma.2007.08.016

42. A. Bratsos, The solution of the two-dimensional sine-Gordon equation using the method of lines, *J. Comput. Appl. Math.*, **206** (2007), 251–277. https://doi.org/10.1016/j.cam.2006.07.002

Appendix

Appendix A: abbreviation list

Abbreviation	Full name
WG	Weak Galerkin
SFWG	Stabilizer Free Weak Galerkin
UWG	Unified Weak Galerkin with or without stabilizer
SWG	simplified weak Galerkin
POD	Proper Orthogonal Decomposition
SG	sine-Gordon
CN	Crank–Nicolson
DG	discontinuous Galerkin
HDG	hybridized discontinuous Galerkin
TDG-STFE	DG time stepping space–time finite element